

# Edge-Directed Invariant Shoeprint Image Retrieval

Lahouari Ghouti, Ahmed Bouridane and Danny Crookes

School of Computer Science, Queen's University of Belfast,  
Belfast BT7 1NN, United Kingdom.

Email: {L.Ghouti, A.Bouridane, D.Crookes}@qub.ac.uk

**Keywords:** Scene of crime evidence, shoeprint images, wavelet maxima, moment-invariant features, Hu and geometric moments.

## Abstract

In this paper, we propose the use of image feature points for the classification of shoeprint images in a forensic setting. These feature points are quantified using wavelet maxima points extracted from a nonorthogonal wavelet decomposition of the shoeprint images. Wavelet transforms have been shown to be an effective analysis tool for image indexing, retrieval and characterization. This effectiveness is mainly attributed to the ability of the latter transforms to capture well the spatial information and visual features of the analyzed images using only few dominant subband coefficients. In this work, we propose the use of a nonorthogonal multiresolution representation to achieve shift-invariance. To reduce the content redundancy, we limit the feature space to wavelet maxima points. Such dimensionality reduction enables compact image representation while satisfying the requirements of the "information-preserving" rule. Based on the wavelet maxima representations, we suggest the use of a variance-weighted minimum distance measure as the similarity metric for image query, retrieval, and search purposes. As a result, each image is indexed by a vector in the wavelet maxima moment space. Finally, performance results are reported to illustrate the robustness of the extracted features in searching and retrieving of shoeprint images independently of position, size, orientation and image background.

## 1 Introduction

Recent developments in forensic science have resulted in large numbers of crime scene images being collected for recording and analysis. Shoeprint images are no exception. Bodziak [1] indicates that shoeprint evidence from crime scenes is more frequently present than fingerprints. In Daubert rulings [2], the US Court upholds, as a general principle, the relevance and reliability of the "science" of footwear impression evidence in criminal cases generally. Girod [3] suggests that 30% of the burglary scenes provide valid evidence and usable shoeprints. Also, 35% of the scenes of crime present shoeprint traces that can be used as scientific evidence in forensic science as reported in a study conducted in several jurisdictions in Switzerland. However, to increase the reliability of decision

making in such forensic settings and assist the forensic specialist in his/her duties, there must be an effective and precise framework for searching, browsing, querying, and interacting with these important collections and such processes are expected to be carried out in a timely manner. In response to these concerns, systems, known as QBIC (Query By Image Content) [4], have been recognized as a potential solution for this fast-growing "digital forensic world". In this paper, we propose the use of image feature points for the classification of shoeprint images in a forensic setting. These feature points are quantified using wavelet maxima points extracted from nonorthogonal wavelet decomposition of the shoeprint images. The paper organization is as follows. Section II describes the basic components of the proposed shoeprint retrieval system. Mathematical details about the nonorthogonal wavelet transform are given. Also, the distance metrics used in this work are described. In Section III, we present the performance results for the shoeprint retrieval system in the presence of various image alterations and manipulations such as additive white Gaussian noise (AWGN), Wiener/median filtering, JPEG compression, scaling and rotation. Conclusions and future work directions are drawn in Section IV.

## 2 The Shoeprint Retrieval System

A nonorthogonal multiresolution decomposition is used to extract the wavelet maxima [5]. The resulting image decomposition is redundant since the latter decomposition does not involve downsampling after each decomposition stage. Fig. 1 shows the decomposition and reconstruction structures of nonorthogonal wavelet transforms. For illustration purposes, we show, in Fig. 2, the approximation subbands of a shoeprint image after three decomposition levels using both types of decompositions (orthogonal and nonorthogonal). Nonorthogonal wavelet transforms are known for their ability to capture the salient signal features (for both 1D and 2D signals) as detailed in [5]. Image edges can be efficiently quantified using such transforms.

### 2.1 Wavelet Maxima Representation

In order to preserve the shift-invariance property, wavelet maxima representations are used for their ability to adapt the sampling scheme by translating the sampling grid when the processed input is translated [5]. Borrowing the underlying principles of Canny's multiresolution edge detector algorithm, let's define two wavelet functions that are partial derivatives of a two-dimensional smoothing function  $\theta(x, y)$  [5]:

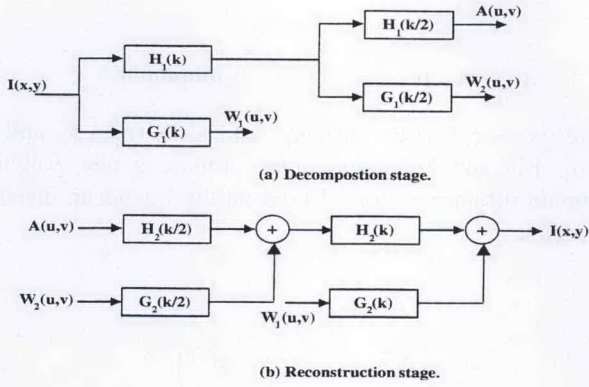


Figure 1: Nonorthogonal wavelet transform. (a) Decomposition stage. (b) Reconstruction stage.

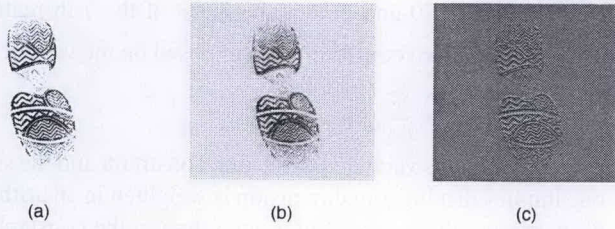


Figure 2: Nonorthogonal wavelet decomposition of a shoeprint image. (a) Shoeprint image. (b) Approximation subband using orthogonal decomposition. (c) Approximation subband using nonorthogonal decomposition.

$$\psi^1(x, y) = \frac{\partial \theta(x, y)}{\partial x} \quad \text{and} \quad \psi^2(x, y) = \frac{\partial \theta(x, y)}{\partial y} \quad (1)$$

Then, the wavelet transform of the input image,  $I(x, y)$ , at a scale  $s = 2^j$  has the following two components:

$$W_x^I(s; u, v) = \int_{-\infty}^{\infty} \int_{-\infty}^{\infty} I(x, y) \psi_s^1(x - u, y - v) dx dy \quad (2)$$

$$W_y^I(s; u, v) = \int_{-\infty}^{\infty} \int_{-\infty}^{\infty} I(x, y) \psi_s^2(x - u, y - v) dx dy \quad (3)$$

where  $W_x^I(s; u, v)$  and  $W_y^I(s; u, v)$  are the wavelet coefficients at location point  $(u, v)$  in the x-channel and y-channel components at scale  $s$ , respectively. Mallat and Zhong [5] show that the two components given in Eqs. 2-3 are proportional to the coordinates of the gradient vector of  $I(x, y)$  smoothed by  $\theta_s(x, y)$ . The modulus and phase of the wavelet transform are given by:

$$M^I(s; u, v) = \sqrt{|W_x^I(s; u, v)|^2 + |W_y^I(s; u, v)|^2} \quad (4)$$

$$A^I(s; u, v) = \arctan \left( \frac{W_y^I(s; u, v)}{W_x^I(s; u, v)} \right) \quad (5)$$

**Hu Moments of Wavelet Maxima Points:** Before applying the similarity metric defined below, we need to find a more compact representation for the extracted wavelet maxima points since the latter characterize a rather "scattered" representation. Invariant image moments are such compact mapping. Image moments have been widely used in pattern recognition applications to represent the shapes of different objects [6]. However, it is worth noting that such moment invariants should not be computed in the same way as with image objects. This difference is mainly attributed to the dense nature of the wavelet maxima points along curves rather than regions [6]. The  $(p + q)^{th}$ -order wavelet maxima moment of the image  $I(x, y)$  is defined as [6]:

$$m_{pq}^s = \sum_{(u,v) \in \mathcal{M}^s} u^p v^q M^I(s; u, v), \quad p, q = 0, 1, 2, \dots \quad (6)$$

where  $\mathcal{M}^s$  denotes the set of all wavelet maxima points of a given image at scale  $s = 2^j$ . A similar relation to Eq. 6 can be defined using the angle  $A^I(s; u, v)$  instead of the modulus  $M^I(s; u, v)$ . However, the moment relation, Eq. 6, contains already the information about the direction of the gradient vectors of the image  $I(x, y)$ . Shift-invariance is guaranteed by centralizing the wavelet maxima points to their center of mass  $(\bar{u}^s, \bar{v}^s)$  where  $\bar{u}^s = \frac{m_{10}^s}{m_{00}^s}$  and  $\bar{v}^s = \frac{m_{01}^s}{m_{00}^s}$ . Therefore, Eq. 6 can be rewritten as:

$$\mu_{pq}^s = \sum_{(u,v) \in \mathcal{M}^s} (u - \bar{u}^s)^p (v - \bar{v}^s)^q M^I(s; u, v), \quad p, q = 0, 1, 2, \dots \quad (7)$$

The moments, defined in Eq. 7, can be further normalized by  $|\mathcal{M}^s|$ , the number of the points in the set  $\mathcal{M}^s$  and their spread factor  $\sqrt{\mu_{20}^s + \mu_{02}^s}$  as follows:

$$\eta_{pq}^s = \frac{\frac{\mu_{pq}^s}{|\mathcal{M}^s|}}{\left( \frac{\mu_{20}^s}{|\mathcal{M}^s|} + \frac{\mu_{02}^s}{|\mathcal{M}^s|} \right)^{\frac{p+q}{2}}} \quad (8)$$

Finally, to account for rotation-invariance, we propose to use seven invariant moments up to the third order as defined in [6] for each decomposition level. Since we are using 4 decomposition levels and 7 invariant moments for each

scale, feature vector consisting of 28 elements will be used in the computation of the similarity metric defined below. Fig. 3 illustrates the reason behind setting the maximum decomposition level to 4. As illustrated, Fig. 3-(b) indicates that the wavelet maxima points at decomposition level 4 retain most of the image contours unlike those at level 5 where some of the edges are lost.

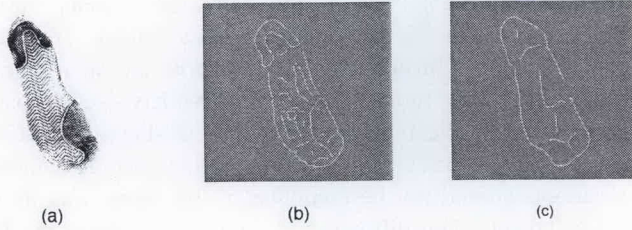


Figure 3: (a) Shoeprint image. (b) Wavelet maxima at decomposition level 4. (c) Wavelet maxima at decomposition level 5.

## 2.2 Similarity Metric

A central concept to the classification of features extracted from shoeprint images is the selection of the appropriate distance measure. A good and intuitive selection of such metric is an essential step towards a successful shoeprint image classification system. Let the data set  $\mathbf{X} = \{\mathbf{x}_1, \mathbf{x}_2, \dots, \mathbf{x}_n\} \in R^m$  be a subset of the real  $m$ -dimensional vector space  $R^m$ . Each element  $\mathbf{x}_i$  is called a feature vector and  $x_{ij}$  represents the  $j$ -th feature of the observation  $\mathbf{x}_i$ . Also, all the patterns to be classified belong to the set  $\mathbf{X}$ . The distance between patterns  $\mathbf{x}_i$  and  $\mathbf{x}_j$  is defined as a real-valued function  $d: \mathbf{X} \times \mathbf{X} \rightarrow R^+$ , such that [6]:

- 1)  $d(x_i, x_j) = d_{ij} \geq 0$ ,    2)  $d_{ij} = 0$  iff  $x_i = x_j$
- 3)  $d_{ij} = d_{ji}$ ,    4)  $d_{ij} \leq d_{ik} + d_{jk}$

Many distance functions have been proposed in the literature [6]. Most of these functions can be cast into two broad classes: 1) probabilistic distance metrics and 2) nonprobabilistic metrics. Probabilistic class includes metrics such as the Bhattacharyya and divergence distances. Such distances are usually used as an information measure of feature effectiveness such that the selected features based on distance criteria will minimize indirectly the probability of misrecognition [6]. Nonprobabilistic distances, such as the Euclidean, the city block (Manhattan), Minkowski, Czekanowski, Hausdorff and Mahalanobis distances are used to measure the dissimilarity between two feature vectors. *Minimum distance* metrics are defined for measuring the distances between the input feature vector and a set of reference vectors in the feature space. Let's define  $c$  reference vectors  $\mathbf{r}_1, \mathbf{r}_2, \dots, \mathbf{r}_c$  with  $\mathbf{r}_i$  associated with the pattern class  $c_i$ . A minimum distance metric, with respect to  $\mathbf{r}_1, \mathbf{r}_2, \dots, \mathbf{r}_c$ , would classify the input pattern  $\mathbf{x}_i$  as belonging to  $c_k$ , i.e. [6]:

$$\mathbf{x}_i \sim c_k \text{ if } \|\mathbf{x}_i - \mathbf{r}_k\| \text{ is minimum,} \quad (9)$$

where  $\|\mathbf{x}_i - \mathbf{r}_k\|$  is the distance defined between  $\mathbf{x}_i$  and  $\mathbf{r}_k$ . In [6], Lin and Venetsanopoulos propose a new weighted minimum distance metric. Based on the Euclidean distance, they define:

$$d_{ki}^2 = \sum_{j=1}^m w_j^{(k)} (x_{ij} - \bar{x}_j^{(k)})^2 \quad (10)$$

where  $w_j^{(k)}$  is the weight for associated with the attribute element in Eq. 10 and  $\bar{x}_j^{(k)}$  is the mean of the  $j$ -th feature in class  $k$ . In [6], two constraints are imposed on the weight  $w_j^{(k)}$ :

$$1) w_j^{(k)} \geq 0 \quad 2) \sum_{j=1}^m w_j^{(k)} = 1$$

and  $w_j^{(k)}$  remains valid due to the first constraint and the second one implies that the  $j$ -th dimension is weighted in an arithmetic proportion to the other features according to the constant sum. Lin and Venetsanopoulos [6] define  $w_j^{(k)}$  as:

$$w_j^{(k)} = \frac{1}{\sigma_j^{2(k)}} \quad (11)$$

where  $\sigma_j^{2(k)}$  is the variance of the  $j$ -th feature of class  $k$ . Such a choice for  $w_j^{(k)}$  enables to distribute small relative weights to features with large variances and large weights are assigned to those features with small variances. Such weight distribution has the effect of equalizing the importance of each feature vector within the same class.

## 3 Simulation Results

In this section, we evaluate the performance of the proposed method in the *query-by-example* approach. Experiments were conducted to assess the system performance using the full shoeprint images. The original database consists of 31 medium and low quality shoeprint images. To evaluate the shift-, scale- and rotation-invariance of the selected features, each shoeprint image in the database, a class of 11 images was constructed by randomly rotating, scaling and pasting that image into a randomly selected background. The scaling factor is a uniform random variable between 0.5 and 1. The pasting position was randomly selected such that the resulting shoeprint image would entirely fit inside the background image. The background images are selected from a set of wooden, soil and snow texture images of size  $256 \times 256$ . Thus, the database

contains 341,  $256 \times 256$  grey-level shoeprint images. Each image in the database was used in the query in order to retrieve the other 10 relevant ones. To illustrate the thresholding effect, Fig. 4 shows the performance of the shoeprint class retrieval (31 classes) using 100%, 60% and 30% of the wavelet maxima points. It is clear that the proposed system is able to correctly classify the shoeprint classes though the percentage of the maximal points drops drastically from 100% to 30%. This robustness is contributed to the projection property of wavelet maxima representation [5]. In Fig. 5, we report the retrieval results for a specific target shoeprint image (image No. 34). As expected, the system yields the smallest metric distance (i.e., highest match) for the query image. Finally, to illustrate the robustness of the proposed system against specific image alterations such as cropping and compression, Fig. 6 shows the retrieval results for the same target image using the upper half part only. Though, the system does not yield the smallest metric for the target image, it succeeds to classify the target as the top-second match.

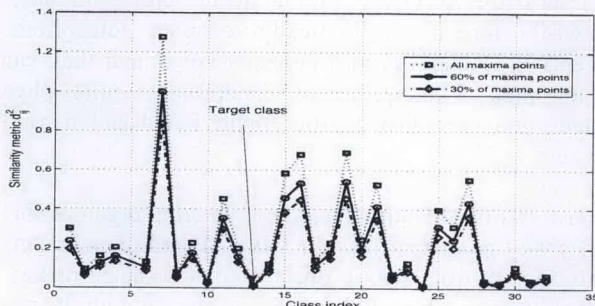


Figure 4: Effect of maxima points' thresholding.

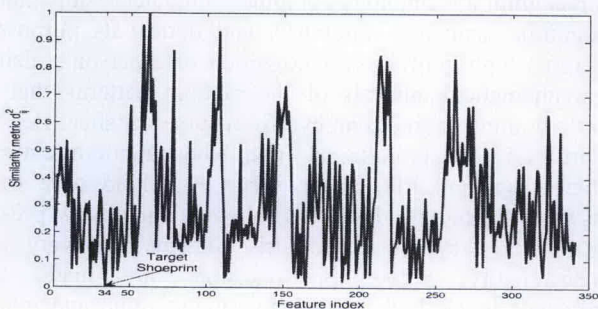


Figure 5: Similarity metric for the classification of shoeprint feature No. 34.

#### 4 Conclusions

In this paper, we have developed a wavelet-based shoeprint image retrieval system that is characterized by high robustness in searching and retrieving shoeprint images independently of position, size, orientation and image background. In order to preserve the shift-invariance property, the proposed system is based on a nonorthogonal wavelet decomposition. However, such a solution is achieved at the expense of increased information redundancy. Therefore, efficient dimensionality reduction is required. Indeed, we compact the multiresolution

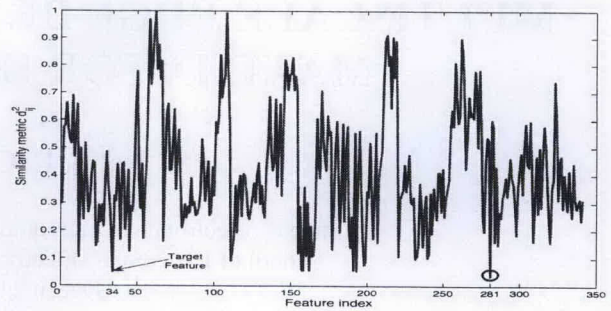


Figure 6: Similarity metric for the classification the shoeprint feature No. 34 using only its upper half part.

representations by constructing feature vectors dependent only on the geometric moments of wavelet maxima points. The obtained representation results in a compact, shift-, rotation-, scale-invariant feature set. Finally, as a possible future extension of the present work, a robust perceptual image hashing scheme may be developed using wavelet maxima as feature points for the construction of perceptually robust hash strings.

#### 5 Acknowledgments

This work is supported by ESPRC Grant No. EP/C008057/1. The authors would like to thank Freeman and Foster Ltd. for providing the shoeprint images.

#### References

- [1] W. J. Bodziak, *Footwear Impression Evidence Detection, Recovery and Examination*. CRC Press, Second Edition, 2000.
- [2] "Daubert Rulings: Footwear Impression Evidence," Apr. 2002. United States District Court - Northern District of Indiana - Fort Wayne Division, USA.
- [3] A. Girod, "Computer classification of the shoeprint of burglar soles," *Forensic Science Int'l*, vol. 82, no. X, pp. 59–65, Sep. 1996.
- [4] M. Flickner, H. Shawney, W. Niblack, J. Ashley, Q. Huang, B. Dom, M. Gorkani, J. Hafner, D. Lee, D. Petkovic, D. Steele, and P. Yanker, "Query by image and video content: The QBIC system," *IEEE Computer*, vol. 49, no. 3, pp. 23–32, Sep. 1995.
- [5] S. Mallat, *A Wavelet Tour of Signal Processing*. Academic Press, Second Edition, 1999.
- [6] M. Do, S. Ayer, and M. Vetterli, "Invariant image retrieval using wavelet maxima moment," in *Proc. 3rd Int. Conf. on Visual Info. and Info. Systems*, pp. 451–458, Amsterdam, Holland, Jun. 1999.